

2026

Establishment of diagnostic markers for differentiation of oral lichen planus and oral erythroleukoplakia with lichenoid features through a transcriptomic profile analysis

Julia Yu Fong Chang

Jung-Tsu Chen

Yi-Ping Wang

Follow this and additional works at: <https://jds.ads.org.tw/journal>

Recommended Citation

Chang, Julia Yu Fong; Chen, Jung-Tsu; and Wang, Yi-Ping (2026) "Establishment of diagnostic markers for differentiation of oral lichen planus and oral erythroleukoplakia with lichenoid features through a transcriptomic profile analysis," *Journal of Dental Sciences*: Vol. 21: Iss. 2, Article 60.
Available at: <https://jds.ads.org.tw/journal/vol21/iss2/60>

This Original Article is brought to you for free and open access by Journal of Dental Sciences. It has been accepted for inclusion in Journal of Dental Sciences by an authorized editor of Journal of Dental Sciences. For more information, please contact cpchiang@ntu.edu.tw.



Available online at <https://jds.ads.org.tw/journal/>

Digital Commons

journal homepage: <https://jds.ads.org.tw/journal/>



Original Article

Establishment of diagnostic markers for differentiation of oral lichen planus and oral erythroleukoplakia with lichenoid features through a transcriptomic profile analysis

Julia Yu Fong Chang^{a,b}, Jung-Tsu Chen^{b,c}, Yi-Ping Wang^{a,b*}

^a Department of Dentistry, School of Dentistry, National Taiwan University, Taipei, Taiwan

^b Department of Dentistry, National Taiwan University Hospital, College of Medicine, National Taiwan University, Taipei, Taiwan

^c Graduate Institute of Clinical Dentistry, School of Dentistry, National Taiwan University, Taipei, Taiwan

Received 12 January 2026

Available online 1 April 2026

KEYWORDS

Oral lichen planus;
Oral erythroleukoplakia with lichenoid features;
NanoString;
Diagnostic markers

Abstract *Background/purpose:* Oral lichen planus (OLP) frequently overlaps clinically and histopathologically with oral erythroleukoplakia (OEL), a high-risk oral potentially malignant disorder. OEL with lichenoid features (OEL-L) may closely mimic OLP, resulting in diagnostic uncertainty and inappropriate management. This study aimed to characterize immune and epithelial transcriptomic differences between OLP and OEL-L and to identify potential diagnostic biomarkers.

Materials and methods: Formalin-fixed paraffin-embedded specimens from 6 OLP and 6 OEL-L cases were analyzed retrospectively. Diagnoses were established according to World Health Organization criteria. Immune and epithelial gene expression profiles were assessed using the NanoString nCounter Autoimmune Discovery and PanCancer Progression panels. Differentially expressed genes were identified using a fold change >5 and $P < 0.01$.

Results: OLP lesions showed marked activation of T-cell-associated immune pathways, including T-cell receptor signaling, natural killer cell cytotoxicity, and type I interferon responses. In contrast, OEL-L exhibited global suppression of adaptive immune signatures with enrichment of metabolic and oxidative stress pathways. OEL-L demonstrated increased expression of B-cell- and plasma cell-related genes [tumor necrotic factor receptor superfamily member 17 (TNFRSF17), CD79A] and epithelial-derived C-X-C motif ligand 8 (CXCL8) and matrix metalloproteinase 12 (MMP12), accompanied by stromal and extracellular matrix-remodeling signatures.

* Corresponding author. Department of Dentistry, National Taiwan University Hospital, College of Medicine, National Taiwan University, No. 1, Chang-Te Street, Taipei, 10048, Taiwan.

E-mail address: ypwang0530@ntu.edu.tw (Y.-P. Wang).

<https://doi.org/10.1016/j.jds.2026.01.016>

1991-7902/© 2026 Association for Dental Sciences of the Republic of China. Publishing services by Digital Commons. This is an open access article under the CC BY-NC-ND license (<http://creativecommons.org/licenses/by-nc-nd/4.0/>).

Conclusion: Distinct immune and epithelial transcriptomic profiles differentiate OLP from OEL-L. CXCL8, MMP12, and B-cell-associated markers may serve as useful adjunctive biomarkers for pathological discrimination.

© 2026 Association for Dental Sciences of the Republic of China. Publishing services by Digital Commons. This is an open access article under the CC BY-NC-ND license (<http://creativecommons.org/licenses/by-nc-nd/4.0/>).

Introduction

Oral lichen planus (OLP) is a relatively common immune-mediated mucocutaneous disease, with a reported global prevalence of up to 5%.¹ Clinically, OLP typically presents as interlacing white striae (Wickham striae) on an erythematous background,^{2,3} although the classic reticular pattern tends to diminish with disease duration. Despite these characteristic features, substantial clinical and histopathological overlap exists between OLP and other oral mucosal disorders, creating significant diagnostic challenges in the routine practice.⁴ Among OLP mimickers, oral erythroleukoplakia (OEL) is of particular concern. OEL is a clinical diagnostic entity representing one of the most severe oral potentially malignant disorders (OPMD), frequently harboring high-grade epithelial dysplasia and carrying a high risk of malignant transformation.⁵ Clinically, OEL often manifests as mixed red-and-white patches or plaques with a smooth or granular surface. According to the World Health Organization, erythroplakia is defined as a “fiery red patch that cannot be characterized clinically or pathologically as any other definable disease.” Although solitary lesions are more typical of OEL than erosive OLP, multifocal OEL is not uncommon, especially in patients with extensive carcinogen exposure due to field cancerization, further complicating the clinical distinction.

Histopathologically, OLP classically demonstrates hyperparakeratosis or hyperorthokeratosis, basal cell degeneration, Civatte body formation, and a band-like lymphocytic infiltrate in the superficial lamina propria.^{6,7} However, basal and parabasal cellular atypia may occasionally be observed, which can mimic epithelial dysplasia. Conversely, epithelial dysplasia and oral squamous cell carcinoma frequently exhibit lichenoid features, including band-like inflammation and basal cell degeneration. Indeed, previous studies have reported focal lichenoid characteristics in nearly one-third of dysplastic or malignant oral lesions, underscoring the diagnostic ambiguity between OLP and OEL with lichenoid features (OEL-L).⁸

Direct immunofluorescence (DIF) is commonly employed to support an OLP diagnosis, with shaggy fibrinogen deposition along the basement membrane zone, which is considered characteristic. Nevertheless, fibrinogen and complement deposition at the basement membrane is not specific for OLP lesions and has also been observed in a substantial proportion of dysplastic and malignant lesions,⁹ limiting its diagnostic utility. Importantly, OLP is typically managed with immunosuppressive therapies, including

corticosteroids and other immunomodulatory agents. Misdiagnosis of OEL-L as OLP may therefore lead to inappropriate immunosuppression, potentially impairing local immunosurveillance and adversely affecting patient outcomes.

Collectively, these challenges highlight a critical unmet need for reliable pathological methods to distinguish OLP from OEL-L. Genome-wide gene expression profiling offers a promising approach to address this issue.^{10,11} By applying the NanoString nCounter system, we aimed to compare immune-related and epithelial gene expression landscapes between OLP and OEL-L lesions, identify pivotal differentially expressed genes, and evaluate their potential as diagnostic biomarkers.

Table 1 Clinical information of 6 enrolled cases of oral lichen planus (OLP) and another 6 enrolled cases of oral erythroleukoplakia with lichenoid features (OEL-L).

Case	Pathological diagnosis	Age	Gender	Location
1	OEL-L/severe dysplasia	57	F	Tongue lateral border
2	OEL-L/moderate to severe dysplasia	75	M	Labial mucosa, lower
3	OEL-L/moderate dysplasia	67	M	Buccal mucosa, left
4	OEL-L/moderate dysplasia	68	M	Buccal mucosa, right
5	OEL-L/severe dysplasia	61	F	Tongue, lateral border
6	OEL-L/moderate dysplasia	46	M	Buccal mucosa, left
7	Lichenoid mucositis	44	F	Buccal mucosa, right
8	OLP	63	F	Tongue lateral border
9	OLP	71	F	Buccal mucosa, right
10	OLP	19	M	Tongue, dorsal surface
11	OLP	60	F	Buccal mucosa, left
12	OLP	28	M	Buccal mucosa, right

Materials and methods

Acquisition of formalin-fixed paraffin-embedded tissue specimens

Formalin-fixed paraffin-embedded (FFPE) tissue specimens of OLP and OEL were retrospectively retrieved from the archives of the Department of Oral Pathology, National Taiwan University Hospital from 2016 to 2020. This study was conducted in accordance with institutional and ethical guidelines and was approved by the Institutional Review Board of National Taiwan University Hospital (IRB No. 202006190RINA). Relevant clinical information was obtained through the chart review. Specimens from patients younger than 20 years of age or with a history of prior treatment were excluded.

Histopathological diagnoses were established based on review of hematoxylin and eosin (H&E)-stained tissue sections, supplemented by DIF findings in OLP cases, according to World Health Organization diagnostic criteria. All cases were independently evaluated by two experienced oral pathologists. OEL cases exhibiting lichenoid features, including band-like or patchy lymphocytic infiltration at the epithelial-lamina propria interface, basal cell liquefaction degeneration, and lymphocytic

exocytosis, were classified as OEL with lichenoid features (OEL-L). Additionally, OLP cases showing epithelial atypia beyond the basal-parabasal layer or premature dyskeratosis within the lower third of the epithelium were reclassified as OEL-L.

Nanostring nCounter mRNA expression analysis

For transcriptomic analysis, 10- μ m FFPE sections were prepared and macrodissected to collect the entire surface epithelium along with the underlying band-like inflammatory infiltrate, guided by the corresponding H&E-stained slides. Total RNA was extracted using the miRNeasy FFPE Kit (Qiagen Taiwan Company Limited, Taipei, Taiwan) following the manufacturer's protocol. RNA quantity and quality were assessed using NanoDrop spectrophotometry and an Agilent BioAnalyzer (Agilent, Santa Clara, CA, USA). Gene expression profiling was performed using the NanoString nCounter platform with the Autoimmune Discovery and PanCancer Progression panels (Agilent). Data analysis was conducted using the nCounter Advanced Analysis module (v2.0.115, Agilent). Differentially expressed genes with a fold change greater than 5 and a *P*-value less than 0.01 were identified before and after sample regrouping and selected as candidate diagnostic markers.

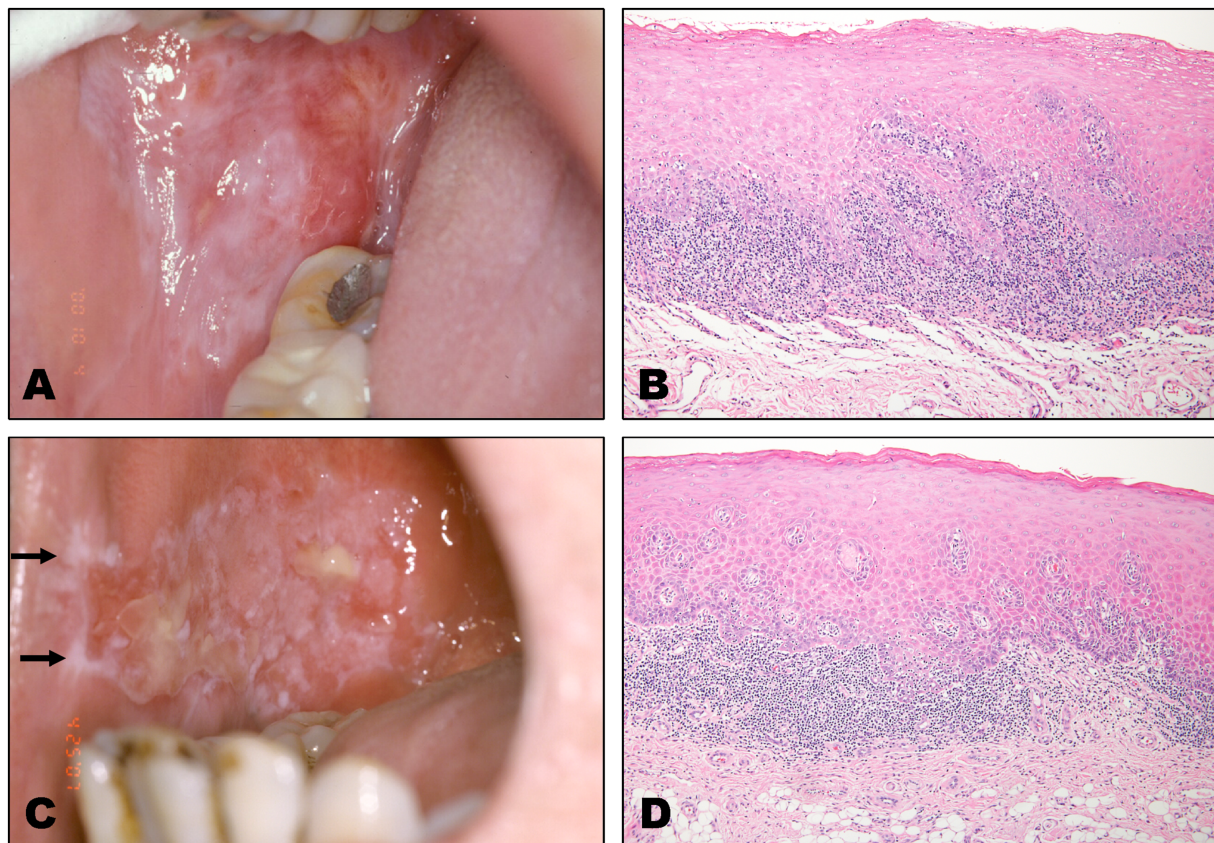


Figure 1 Significant overlapping of clinical presentation and microscopic features between the oral lichen planus (OLP) (A and B, case 4) and oral erythroleukoplakia with lichenoid features (OEL-L) (C and D, case 9). Both diseases appear as intermixed red and white patch to plaque with surface erosion to ulceration grossly. Please note the Whickham striation-like white lines at the anterior border of the OEL-L (C, arrows). A band-like chronic inflammatory cell infiltrate with lymphocytic exocytosis is also discerned in both diseases (B and D).

Results

After reviewing the clinicopathological features and histological slides, 6 cases of OLP and another 6 cases of OEL-L were enrolled for analysis. The information of enrolled 12 cases is summarized in Table 1. The clinical presentation of both entities shared a striking resemblance, which demonstrated intermixed white striation to patch and erythematous to erosive areas (Fig. 1). The mean age of OLP group was approximately a decade younger than that of OEL-L group (47.8 years and 62.3 years, respectively), and a female predilection in the OLP group was discerned. These findings were consistent with previous epidemiology data of both entities,¹² confirming the representativity of enrolled cases. All the males in the OEL-L group had at least one habitual carcinogen consumption, in contrast, the females in this group lacked such exposure. Noteworthy, the OEL-L lesions of both females were located at the lateral border of the tongue.

After microdissection aided with H&E stains, the superficial lamina propria harboring the dense inflammatory cell infiltrate were interrogated with Nanostring Autoimmune Discovery panel, and epithelial components of specimens were subject to Nanostring PanCancer Progression panel analysis. First, we interrogated the immune cell profiles in both groups for comparison. A hierarchical clustering heatmap in regard of the inflammatory cell infiltrates in both groups was generated to illustrate the relative activity of curated immune, inflammatory, and stress-response pathway signatures across all samples (Fig. 2). Each column represented one pathway signature and each row represented an individual sample. Color intensity reflected the normalized enrichment score (NES or Z-score), with yellow indicating the higher pathway activity and blue indicating the lower activity. Both samples and pathways were clustered using unsupervised hierarchical clustering (Euclidean distance, complete linkage), revealing distinct molecular subclasses. The majority of OLP (4 out of 6) displayed marked upregulation of T-cell activation, T cell receptor (TCR) signaling, natural killer (NK)-cell cytotoxicity, and cytokine–cytokine receptor interactions, alongside enriched inflammatory response and type I interferon signaling programs. The concerted induction of IL-6, tumor necrosis factor (TNF), and interferon (IFN)-related pathways indicates a highly inflamed microenvironment characterized by both innate and adaptive immune engagement. Upregulation of antigen presentation pathways further suggests enhanced interactions between antigen-presenting cells and effector lymphocytes. Collectively, this profile reflected a cytotoxic, T-cell–inflamed state commonly associated with increased immune cell infiltration. In contrast, the OEL-L specimens demonstrated widespread suppression of immune-related pathways. These samples exhibited the low activity of T-cell and NK-cell signaling modules, the diminished IFN- α/β and inflammatory cytokine responses, and the reduced enrichment of Th1/Th2/Th17 differentiation pathways. The parallel downregulation of multiple adaptive immune signatures suggest the limited T-cell priming, reduced cytotoxic potential, and a generally immunosuppressed or immune-excluded microenvironment. The relative increases in oxidative stress and metabolic pathways within this cluster

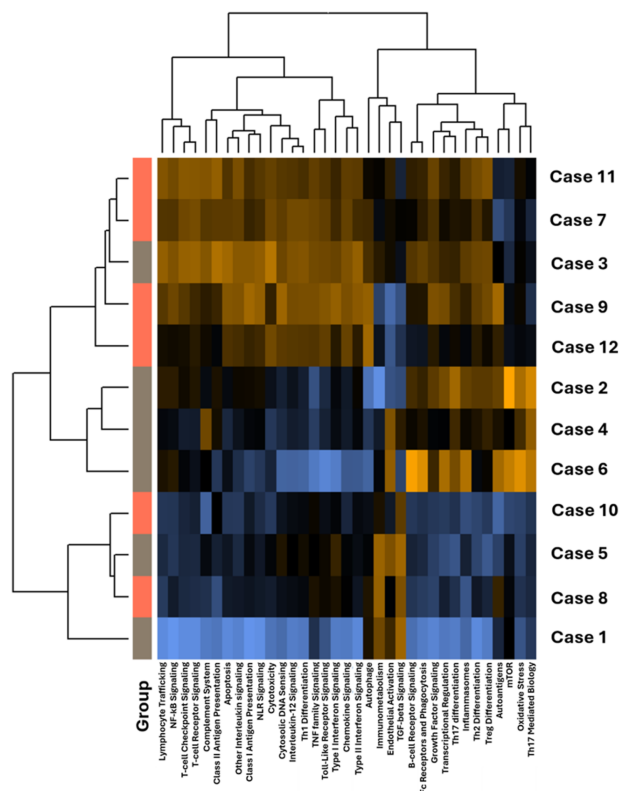


Figure 2 Heatmap analysis on transcriptomic comparison between the immunologic landscapes of the oral lichen planus (OLP) and oral erythroleukoplakia with lichenoid features (OEL-L) ($n = 6$ in each group, Autoimmune Discovery panel). Note the majority of OLP (4 out of 6 cases) manifest a similar transcriptomic profile, e.g., upregulation of NF- κ B axis, T cell receptor signaling, Toll-like receptor (TLR) pathway, IL-12 regulations, etc. These signatures are down-regulated in most OEL-L specimens (5 out of 6 cases). Most importantly, one case previously diagnosed OEL-L displays the profile of OLP and 2 cases with an original diagnosis of OLP manifest the landscape of OEL-L, indicating microscopic evaluation might not be a reliable surrogate of the nature of the diseases. Group: orange, OLP; gray, OEL-L.

pointed to metabolic reprogramming, which might further impede effective immune infiltration or activation through the nutrient competition or hypoxia-driven immunosuppression. To delineate transcriptional differences between OEL-L and baseline LP, we performed the differential expression analysis and visualized the results using a volcano plot (Fig. 3). A pronounced asymmetry toward the upregulated genes was observed, indicating the widespread transcriptional activation in OPMD. Several genes exceeded both statistical significance and fold-change thresholds, highlighting the robust immune and inflammatory responses associated with the disease state. Among the most significantly upregulated transcripts were pro-platelet basic protein (PPBP, which encodes chemokine C-X-C motif ligand 7/CXCL7), tumor necrotic factor receptor superfamily member 17 (TNFRSF17), lymphotoxin beta (LTB), C-X-C motif ligand 8 (CXCL8, which encodes interleukine 8/IL-8), C-X-C motif ligand 3 (CXCL3), CD79A, interferon regulatory

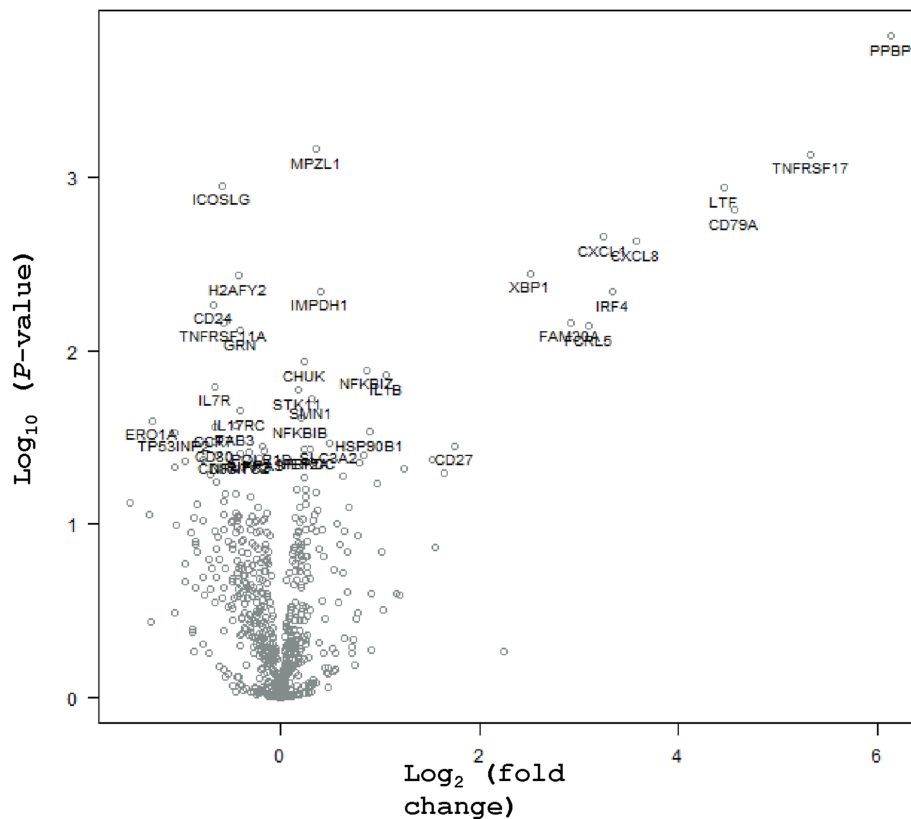


Figure 3 Volcano plot on pilot small-scale transcriptomic comparison between the immunologic landscapes of the oral lichen planus (OLP) and oral erythroleukoplakia with lichenoid features (OEL-L) (n = 6 in each group, Autoimmune Discovery panel, manifested as OEL-L v.s. baseline of OLP).

factor 4 (IRF4), and X-box binding protein 1 (XBP1, encodes a transcriptional factor regulating major histocompatibility complex/MHC class II genes), with \log_2 fold-changes ranging from approximately 2 to 6. These genes were enriched in pathways related to the chemokine production, B-cell receptor (BCR) signaling, plasma cell differentiation, and nuclear factor kappa-light-chain-enhancer of activated B cells (NF- κ B) transcriptional activity. Notably, the upregulation of IRF4, XBP1, and TNFRSF17 marks a transcriptional signature characteristic of activated or post-germinal center B cells and antibody-secreting plasma cells. The increased expression of chemotactic cytokines such as CXCL8 and CXCL3 further suggest the enhanced recruitment of neutrophils and other innate immune cells. Together, these changes indicate a transition toward a highly inflammatory and lymphoid-rich microenvironment that distinguishes OEL-L from baseline LP. In contrast, the downregulated genes were fewer in number and displayed the lower fold changes, with the limited clustering of functional categories. These downregulated transcripts likely reflected a reduction in homeostatic epithelial signaling as inflammatory and immune-mediated processes became dominant in OEL-L.

Next, we investigated the differentially expressed genetic backgrounds in the epithelial component of both groups. The unsupervised hierarchical clustering of curated gene-expression signatures clearly separated the cohort into distinct transcriptional subgroups (Fig. 4). The

dominant axis of variation opposed a mesenchymal/extracellular matrix (ECM)-remodeling program to a proliferation-driven program. One major sample cluster (cases 1, 5, 8, and 10) showed coordinated upregulation of mesenchymal and ECM-related signatures, including mesenchymal transition, ECM organization and receptor interaction, collagen formation, integrin signaling, and metastasis-associated pathways. These lesions simultaneously displayed the reduced activity of cell-cycle and DNA replication signatures. This pattern was consistent with a mesenchymal, ECM-high phenotype, suggestive of an abundant reactive stroma or enhanced invasive potential. In contrast, a second major sample cluster was characterized by strong activation of proliferation-associated signatures, encompassing cell-cycle regulation, G2/M checkpoint control, DNA replication and repair, and chromosomal instability programs. In these lesions, epithelial-mesenchymal transition (EMT)- and ECM-related signatures were comparatively attenuated. This profile was compatible with a proliferation-high, epithelial-like phenotype, in which rapid cell division and replication stress represented the predominant biological features. A third, smaller group (case 2, 9, and 12) displayed intermediate levels of both EMT and proliferation signatures but showed the relatively higher enrichment for immune- and metabolism-related pathways, including inflammatory response, cytokine signaling, and oxidative phosphorylation-associated signatures. This subgroup

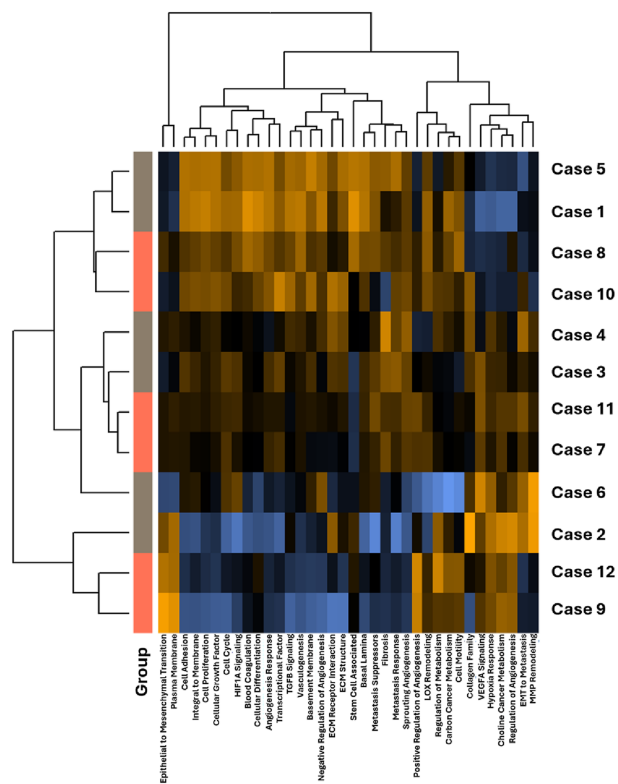


Figure 4 Heatmap analysis on epithelial transcriptomic comparison between the oral lichen planus (OLP) and oral erythroleukoplakia with lichenoid features (OEL-L) (n = 6 in each group). No overt segregation between OLP and OEL-L is discerned. Group: orange, OLP; gray, OEL-L.

likely represented a mixed immune/metabolic phenotype, with transcriptional contributions from both epithelial cells and immune or stromal components of the microenvironment. The volcano plot (Fig. 5) showed a relatively conservative transcriptomic shift, with most genes clustering around a log₂ fold change (FC) of 0 and exhibiting the modest statistical significance. Despite the limited number of transcripts surpassing strict adjusted *P*-value thresholds, several genes displayed noteworthy fold changes consistent with biologically relevant pathway perturbations. A subset of inflammatory and stromal-related transcripts was prominently upregulated in OEL-L. Among these, CXCL8 (IL-8) showed the greatest magnitude of induction (log₂FC ≈ 4), suggesting a marked enhancement of neutrophil-associated chemokine signaling. Additional upregulated genes included cytochrome P450 family 1 subfamily B member 1 (CYP1B1), matrix metalloproteinase 12 (MMP12), pyruvate dehydrogenase kinase 1 (PDK1), pyruvate dehydrogenase kinase 4 (PDK4), asporin (ASPN), insulin like growth factor 1 (IGF1), and Thy-1 cell surface antigen (THY1), reflecting the activation of oxidative metabolism, ECM remodeling, and fibroblast-associated programs. In contrast, the downregulated transcripts were fewer and generally exhibited lower effect sizes. Moderate decreases in CD74, complement C1q B Chain (C1QB), serpin family E member 1 (SERPINE1), erb-b2 receptor tyrosine kinase 4 (ERBB4), and mitogen-activated

protein kinase kinase 1 (MAP2K1) suggest attenuation of antigen presentation mechanisms and immune regulatory signaling. Collectively, these patterns reflect a preferential activation of inflammatory and stromal modules accompanied by subtle suppression of adaptive immune pathways.

Discussion

Autoimmune responses to the altered epithelial antigens or molecular mimicry of antigen of microorganisms are proposed as pathogenetic events of OLP but have not confirmed yet.^{13,14} Previous studies indicated that type 1 immune reaction is responsible for the damage of oral mucosal surface epithelium in OLP.^{15,16} This reaction is driven by soluble factors such as interferons, IL-12, TNF- α , and the cellular components are plasmacytoid and myeloid dendritic cells,¹⁷ and CD4⁺ and CD8⁺ T cells.^{18,19} No evidence of participation of B lymphocytes and antibodies is observed. However, the exact trigger and comprehensive analysis of the immune landscape of OLP have not yet been identified. In addition, the epithelial alteration in OLP is not fully understood and its contribution to the pathogenesis and if these changes confer potential transformation of OLP are still shrouded in mystery. Various studies have investigated carcinogenic molecular events in OLP, such as the telomerase activity, cytogenetic abnormalities, expression of p53, mouse double minute 2 homolog (MDM2), p21, small ubiquitin like modifier 1 (SUMO-1), proliferating cell nuclear antigen (PCNA), argyrophilic nucleolar organizer regions (AgNOR), Ki-67, B-cell lymphoma-2 (Bcl-2), Bcl-2-associated X protein (BAX), and loss of heterozygosity at the tumor suppressor gene loci.^{20–25} However, the results of these studies have not shown convincing and clear evidence of premalignant potential as that is discerned in epithelial dysplasia. A recently published meta-analysis and systemic review of malignant transformation rates of OLP evaluating 16 studies with a total of 7806 patients reported an overall average malignant transformation rate of 1.09%.²⁶ However, the debate about whether OLP should be considered a premalignant condition is still not settled. The two major challenges underlying this issue are as follows: first, important clinical information and/or histopathologic evidence are often missing in publications; second, many other oral diseases may show clinical and microscopic features similar to those found in OLP, and no widely accepted diagnostic criteria for OLP have been articulated yet. Absence of broad consensus in diagnostic criteria of OLP leads to mis-inclusion of different diseases into the same category, and it undermines of the credibility of meta-analysis of the previous studies.

In the present study, we utilized Nanostring nCounter mRNA expression analysis to explore the major epithelial and immunological transcriptomic landscapes between OLP and OEL-L lesions. Combining these two sets, we found that the increased expression of epithelium-derived CXCL8 and MMP12 and enrichment of B cell population (TNFRSF17 and CD79a) in the OEL-L/ED group than those in the OLP group. CXCL8 encodes the precursor of IL-8, which is a prototypical chemokine belonging to the CXC family responsible for the recruitment and activation of neutrophils and granulocytes to the site of inflammation. CXCL8 is almost undetectable

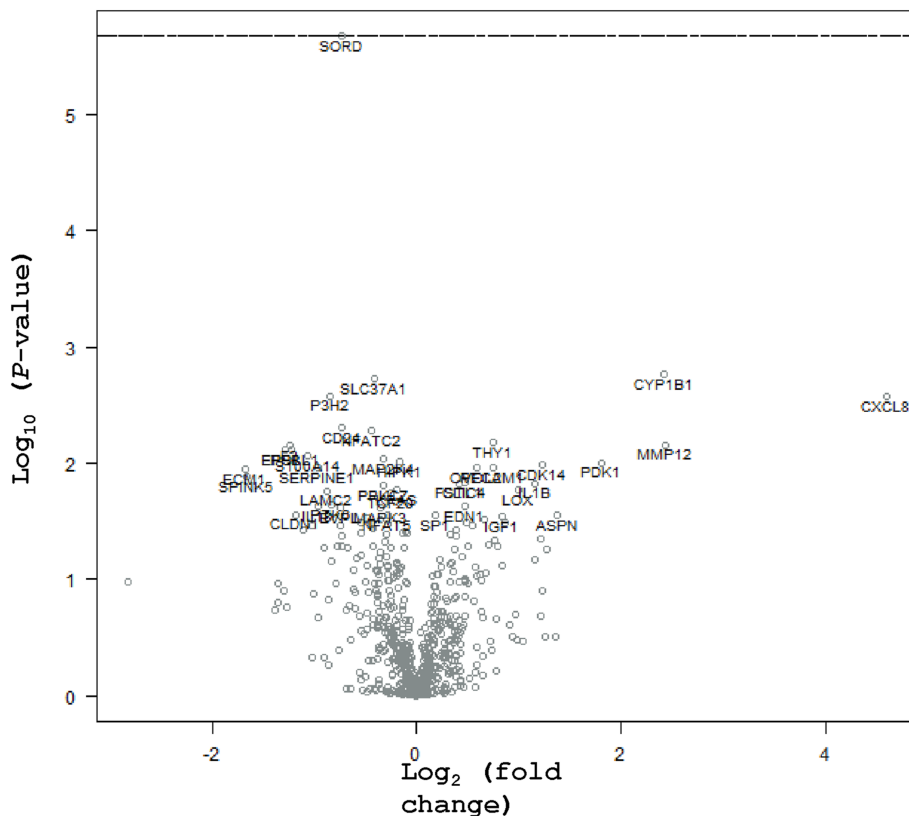


Figure 5 Volcano plot on epithelial transcriptomic comparison between the oral lichen planus (OLP) and oral erythroleukoplakia with lichenoid features (OEL-L) (n = 6 in each group, PanCancer Progression panel, manifested as OEL-L v.s. baseline of OLP).

in physiological states, but is rapidly induced by pro-inflammatory cytokines such as TNF- α and IL-1 β .²⁷ The mechanism of CXCL8-CXCR1/2 signaling in tumorigenesis and tumor progression has been explored extensively. CXCL8 is typically known to promote angiogenesis, but it also activates matrix metalloproteinase (MMP) that is involved in metastasis-related tissue remodelling.^{28,29} MMP12 is a protease involved in macrophage migration, and it also has a crucial role in regulating the resolution of inflammation. MMP12 cleaves IFN- γ , thereby rendering the cytokine unable to signal via its receptor. MMP12 efficiently inactivates IFN- γ by two C-terminal cleavages that remove the IFN- γ receptor-binding site. These cleavages halt the downstream signaling and classical-activation to M1 (IFN- γ -activated) macrophages. M2 macrophages express > 3-fold more MMP12 than the pro-inflammatory M1 macrophages. This suggests a new feedback inhibition mechanism executed by M2 cells that reduces the ratio of destructive M1 cells and so favors tumor-promoting M2 cells.³⁰ These data warrant further investigation of the ratio of T/B cells and the cut-off points of CXCL8 and MMP12 in larger cohorts of OLP and OEL-L.

Declaration of competing interest

The authors have no conflicts of interest relevant to this article.

Acknowledgments

The current study was supported by the grants from National Taiwan University Hospital (NTUH: 114-S0024 and 114-S0258 to Julia Yu Fong Chang and 110-S5055 to Yi-Ping Wang) and the grants from National Science and Technology Council in Taiwan (NSTC 112-2314-B-002-090-MY3 and NSTC 113-2314-B-002-070 to Julia Yu Fong Chang, and NSTC 113-2314-B-002-070 and 114-2314-B-002-095-MY2 to Yi-Ping Wang).

References

1. Gorouhi F, Davari P, Fazel N. Cutaneous and mucosal lichen planus: a comprehensive review of clinical subtypes, risk factors, diagnosis, and prognosis. *Sci World J* 2014;2014:742826.
2. Au J, Patel D, Campbell JH. Oral lichen planus. *Oral Maxillofac Surg Clin North Am* 2013;25:93–100.
3. Crincoli V, Di Bisceglie MB, Scivetti M, Lucchese A, Tecco S, Festa F. Oral lichen planus: update on etiopathogenesis, diagnosis and treatment. *Immunopharmacol Immunotoxicol* 2011;33:11–20.
4. Muller S. Oral lichenoid lesions: distinguishing the benign from the deadly. *Mod Pathol* 2017;30:S54–67.
5. Warnakulasuriya S, Johnson NW, van der Waal I. Nomenclature and classification of potentially malignant disorders of the oral mucosa. *J Oral Pathol Med* 2007;36:575–80.

6. Burgdorf WH, Plewig G. Who described Civatte bodies? *J Cutan Pathol* 2014;41:340–6.
7. Cheng YS, Gould A, Kurago Z, Fantasia J, Muller S. Diagnosis of oral lichen planus: a position paper of the American Academy of Oral and Maxillofacial Pathology. *Oral Surg Oral Med Oral Pathol Oral Radiol* 2016;122:332–54.
8. Fitzpatrick SG, Honda KS, Sattar A, Hirsch SA. Histologic lichenoid features in oral dysplasia and squamous cell carcinoma. *Oral Surg Oral Med Oral Pathol Oral Radiol* 2014;117:511–20.
9. Montague LJ, Bhattacharyya I, Islam MN, Cohen DM, Fitzpatrick SG. Direct immunofluorescence testing results in cases of premalignant and malignant oral lesions. *Oral Surg Oral Med Oral Pathol Oral Radiol* 2015;119:675–83.
10. Glas AM, Kersten MJ, Delahaye LJ, et al. Gene expression profiling in follicular lymphoma to assess clinical aggressiveness and to guide the choice of treatment. *Blood* 2005;105:301–7.
11. Lamb J, Crawford ED, Peck D, et al. The connectivity map: using gene-expression signatures to connect small molecules, genes, and disease. *Science* 2006;313:1929–35.
12. Speight PM, Khurram SA, Kujan O. Oral potentially malignant disorders: risk of progression to malignancy. *Oral Surg Oral Med Oral Pathol Oral Radiol* 2018;125:612–27.
13. Lodi G, Scully C, Carrozzo M, Griffiths M, Sugerman PB, Thongprasom K. Current controversies in oral lichen planus: report of an international consensus meeting. Part 2. Clinical management and malignant transformation. *Oral Surg Oral Med Oral Pathol Oral Radiol Endod* 2005;100:164–78.
14. Payeras MR, Cherubini K, Figueiredo MA, Salum FG. Oral lichen planus: focus on etiopathogenesis. *Arch Oral Biol* 2013;58:1057–69.
15. Santoro A, Majorana A, Bardellini E, Festa S, Sapelli P, Facchetti F. NF-kappaB expression in oral and cutaneous lichen planus. *J Pathol* 2003;201:466–72.
16. Lage D, Pimentel VN, Soares TC, Souza EM, Metze K, Cintra ML. Perforin and granzyme B expression in oral and cutaneous lichen planus - a comparative study. *J Cutan Pathol* 2011;38:973–8.
17. Santoro A, Majorana A, Roversi F, et al. Recruitment of dendritic cells in oral lichen planus. *J Pathol* 2005;205:426–34.
18. Iijima W, Ohtani H, Nakayama T, et al. Infiltrating CD8+ T cells in oral lichen planus predominantly express CCR5 and CXCR3 and carry respective chemokine ligands RANTES/CCL5 and IP-10/CXCL10 in their cytolytic granules: a potential self-recruiting mechanism. *Am J Pathol* 2003;163:261–8.
19. Hu JY, Zhang J, Cui JL, et al. Increasing CCL5/CCR5 on CD4+ T cells in peripheral blood of oral lichen planus. *Cytokine* 2013;62:141–5.
20. O'Flatharta C, Leader M, Kay E, et al. Telomerase activity detected in oral lichen planus by RNA in situ hybridisation: not a marker for malignant transformation. *J Clin Pathol* 2002;55:602–7.
21. Kim J, Yook JI, Lee EH, et al. Evaluation of premalignant potential in oral lichen planus using interphase cytogenetics. *J Oral Pathol Med* 2001;30:65–72.
22. Zhang L, Cheng X, Li Y, et al. High frequency of allelic loss in dysplastic lichenoid lesions. *Lab Invest* 2000;80:233–7.
23. Acay RR, Felizzola CR, de Araujo N, de Sousa SO. Evaluation of proliferative potential in oral lichen planus and oral lichenoid lesions using immunohistochemical expression of p53 and Ki67. *Oral Oncol* 2006;42:475–80.
24. Oliveira Alves M, Balducci I, Rodarte Carvalho Y, Cabral L, Nunes F, Almeida J. Evaluation of the expression of p53, MDM2, and SUMO-1 in oral lichen planus. *Oral Dis* 2013;19:775–80.
25. Pigatti FM, Taveira LA, Soares CT. Immunohistochemical expression of Bcl-2 and Ki-67 in oral lichen planus and leukoplakia with different degrees of dysplasia. *Int J Dermatol* 2015;54:150–5.
26. Fitzpatrick SG, Hirsch SA, Gordon SC. The malignant transformation of oral lichen planus and oral lichenoid lesions: a systematic review. *J Am Dent Assoc* 2014;145:45–56.
27. Hoffmann E, Dittrich-Breiholz O, Holtmann H, Kracht M. Multiple control of interleukin-8 gene expression. *J Leukoc Biol* 2002;72:847–55.
28. Azenshtein E, Meshel T, Shina S, Barak N, Keydar I, Ben-Baruch A. The angiogenic factors CXCL8 and VEGF in breast cancer: regulation by an array of pro-malignancy factors. *Cancer Lett* 2005;217:73–86.
29. Kim SJ, Uehara H, Karashima T, McCarty M, Shih N, Fidler IJ. Expression of interleukin-8 correlates with angiogenesis, tumorigenicity, and metastasis of human prostate cancer cells implanted orthotopically in nude mice. *Neoplasia* 2001;3:33–42.
30. Dufour A, Bellac CL, Eckhard U, et al. C-terminal truncation of IFN-gamma inhibits proinflammatory macrophage responses and is deficient in autoimmune disease. *Nat Commun* 2018;9:2416.